BEST AVAILABLE IMAGES

Defective images within this document are accurate representations of the original documents submitted by the applicant.

Defects in the images may include (but are not limited to):

- BLACK BORDERS
- TEXT CUT OFF AT TOP, BOTTOM OR SIDES
- FADED TEXT
- ILLEGIBLE TEXT
- SKEWED/SLANTED IMAGES
- COLORED PHOTOS
- BLACK OR VERY BLACK AND WHITE DARK PHOTOS
- GRAY SCALE DOCUMENTS

IMAGES ARE BEST AVAILABLE COPY.

As rescanning documents *will not* correct images, please do not report the images to the Image Problem Mailbox.

10/748,822

מדינת ישראל
STATE OF ISRAEL

Ministry of Justice
Patent Office

משרד המשפטים
לשכת הפטנטים

This is to certify that annexed hereto is a true copy of the documents as originally deposited with the patent application of which particulars are specified on the first page of the annex.

זאת לתעודה כי רצופים בזה העתקים נכונים של המסמכים שהופקדו לכתחילה עם הבקשה לפטנט לפי הפרטים הרשומים בעמוד הראשון של הנספח.

This 09-02-2004 היום

רשם הפטנטים
Commissioner of Patents

נתאשר
Certified

חוק הפטנטים, התשכ"ז - 1967
PATENTS LAW, 5727-1967

לשימוש הלשכה
For Office Use

בקשה לפטנט

Application for Patent

מספר: Number:	153731
תאריך: Date:	29-12-2002
הוקדם / נדחה: Ante / Post-dated:	

אני, (שם המבקש, מענו - ולגבי גוף מאוגד - מקום התאגדותו)
I (Name and address of applicant, and, in case of body corporate place of incorporation)

חיים ניב
רחוב שבו 4
הוד השרון 45041
ישראל

Haim Niv
4 Shabo Street
Hod Hasharon 45041
Israel

בעל אמצאה מכח אמצאה Owner, by virtue of

ששמה הוא Inventorship
Of an invention, the title of which is

(בעברית) (Hebrew): חיישן למניעת התקלות במכשולים ובפני הקרקע עבור הליקופטרים וכלי טיס אחרים

(באנגלית) (English): Obstacle and Terrain Avoidance Sensor for Helicopters and Other Aircraft

מבקש בזאת כי ינתן לי עליה פטנט
Hereby apply for a patent to be granted to me in respect therof

*דרישה דין קדימה Priority Claim			*בקשת פטנט מוסף - Application for Patent Addition	*בקשת חלוקה - Application of Division
מדינת האגוד Convention Country	תאריך Date	מספר/ סימן Number/Mark	*לבקשה/לפטנט to Patent/Appl.	מבקשת פטנט from Application
			מס' No.	מס' No.
			מיום Dated	מיום Dated

*יפוי כח: כללי/מיוחד - רצוף בזה/עוד יוגש
P.O.A: general / individual - attached / to be filed later

הוגש בעניין filed in case

המען למסירת הודעות ומסמכים בישראל
Address for Service in Israel

פנסטר ושות'
עורכי פטנטים בע"מ
רח' בזל 16 פ"ת
ת.ד 10256 פ"ת 49002

חתימת המבקש
Signature of Applicant

עבור המבקש,

פנסטר ושות'
עורכי פטנטים בע"מ

היום 29 בחודש דצמבר שנת 2002
This Of the year

לשימוש הלשכה
For Office Use

357/02921

טופס זה, כשהוא מוטבע בחותם לשכת הפטנטים ומושלם מספר ובתאריך ההגשה, הינו אישור להגשת הבקשה שפרטיה רשומים לעיל.
This form, impressed with the Seal of the Patent Office and indicating the number and date of filing, certifies the filing of the application, the particulars of which are set out above.

חיישן למניעת התקלות במכשולים ובפני הקרקע עבור הליקופטרים וכלי טיס אחרים

Obstacle and Terrain Avoidance Sensor for Helicopters and Other Aircraft

חיים ניב

Haim Niv
c:357/02921

OBSTACLE AND TERRAIN AVOIDANCE SENSOR FOR HELICOPTERS AND OTHER AIRCRAFT

1. ABSTRACT

The sensor is a low power, low probability of intercept (LPI) radar, meant to provide terrain avoidance (TA), obstacle avoidance (OA) and warning against controlled flight into terrain (CFIT). Unlike most other sensors conceived for these purposes, it does not use real beam mapping. Instead, it uses Doppler spectrum analysis to generate a set of Doppler filters, representing, each, a cone (A common and usable way to perform the spectral analysis is the Fast Fourier Transform - FFT. Throughout this application, "FFT" will be used instead of "spectral analysis", for ease and simplicity of expression. It should be understood though that other ways to perform spectral analysis can be used also). The cone's head is at the sensor's antenna, its axis coincides with the line of flight (LOF, see Appendix A) and its head angle, 2α is determined by the specific Doppler frequency of the filter. In addition, each conical surface has a width, related to the bandwidth of the Doppler filter (Fig. 5). The conical surfaces intersect with range spheres, resulting in a division of the terrain into many small range-Doppler cells. The azimuth of each cell, θ, is measured, or looked up from a table, using a conventional direction finding (DF) means along with a null in the antenna patterns, directed to a symmetrical range-Doppler cell. The elevation angle of the cell, ϕ, is calculated or looked up from a table, using θ and α, and involves also an ambiguity resolution. At this stage all three coordinates - azimuth, elevation and range are known for each terrain cell or point obstacle, and a three dimensional (3D) map or a set of sky-line contours of the terrain can be generated and displayed. Specific warnings against CFIT can be generated based on the angular distance of the LOF from points in the 3D map or contours.

Point obstacles, such as pylons, trees and structures are also detected by the sensor. Each such obstacle is displayed with its angular distance from the LOF, azimuth, elevation and range.

This principle eliminates the need for a scanning, narrow beam antenna, which requires a combination of large aperture and a very high operating frequency, resulting in a high cost. The current invention uses instead a broad beam, small aperture antenna array, and can operate at lower frequencies. Lower frequencies, in turn, provide better penetration of rain, fog, smoke and dust. An additional feature of the Doppler spectrum analysis is coherent integration, which results in a reduction of the required transmitted power, constituting a low probability of intercept (LPI) feature - desirable especially for military aircraft.

Basically, the sensor uses a Doppler beam sharpening (DBS, Ref. 6) scheme, which has been extended to the vertical axis. In an alternative embodiment, elevation is measured conventionally, and azimuth is computed from it and from the Doppler.

A simpler version of the sensor eliminates azimuth measurement and elevation calculation altogether, (except for a crude azimuth measurement, in a variation of the embodiment). It provides safety circles, allowing the crew to know about a collision hazard and avoid it.

A sensor built according to the invention can include also features and hardware of a wire detection system, as described in US patent 6,278,409 (by Mark Zuta). These will add detection and recognition of suspended wires such as high voltage power lines and warning

against wire strikes. The combination of the above and current inventions would allow also measuring and displaying of the height of the wires.

Otherwise, the sensor will have a limited capability of its own to detect wires and classify them as such.

2. BACKGROUND AND PRIOR ART

CFIT and collision with obstacles account for a large percentage of helicopter and other aircraft accidents, especially at night and adverse weather. The need for a device that would provide adequate warning against obstacles and CFIT for military aircraft is well known. The need exists also for commercial aircraft which are required to fly low, take off from, and land at unprepared and unknown sites, frequently at night and in adverse weather - such as medical evacuation (MEDEVAC), search and rescue (S&R) and police helicopters.

Many schemes have been devised in order to provide the required warnings. Most of these can be divided into two categories:

- Systems which rely on an accurate navigation system - such as the global positioning system (GPS) - and a stored data base of the terrain. An example is the enhanced ground proximity warning system (EGPWS) made by Honeywell. The main shortcoming of this category for helicopters is that there is no assurance that the database is up to date and that there is no new obstacle (such as a pole) that has just recently been erected and does not appear in the database. Another shortcoming of the category is the reliance on GPS or a comparable navigation system, which may not always be available, or in the case of a military mission, might be jammed.

- Systems which rely on real beam mapping, such as millimeter wave (MMW) or laser radars. Examples include MMW radars from Honeywell and Thomson-CSF, and laser radars from Northrop [ref. 1] and Fibertek [ref. 2]. The last two were developed for the US army "OASYS" program, but have not been procured. This category has the following shortcomings:

  - both MMW and laser sensors have been using mechanical scanning, which contributes to high cost, high weight and low reliability.
  - the high frequency (MMW or laser) requires expensive components.
  - the high frequency radiation does not penetrate well rain, fog, smoke and dust.
  - Laser has a difficulty looking into, or close to the direction of the sun

In fighters and other aircraft, DBS has been used for mapping in a horizontal plane. The current invention uses DBS, along with a relation among azimuth, elevation and Doppler, to obtain also elevation, allowing 3D mapping.

A unique method which also uses radar with Doppler spectrum analysis, is described in Russian patent RU 2128846 [ref . 3]. This method uses a different approach, providing the **height** of discrete obstacles, which is measured through the **width** of a Doppler spectrum. Contrary to this approach, the current invention uses measured Doppler values to directly obtain elevation angles of terrain cells, obstacle tips and other parts of obstacles. Moreover, the Russian patent method does not provide 3D mapping of the terrain in front

of the aircraft, nor does it address obstacles and terrain features which extend above the flight plane (see app. A for definition of flight plane).

Another method for elevation measurement, based on Doppler and azimuth is described in US patent 5,847,673 [ref. 4]. It uses a narrow, steerable antenna beam, and a different formula to calculate elevation. It obtains object coordinates by first calculating it in antenna coordinates, then transforming it to aircraft or inertial coordinates. Mapping or terrain avoidance are not mentioned. Contrary to this approach, the current invention uses broad antenna beams to directly obtain elevation angles of obstacles and terrain features, and generate a 3D map or terrain contours.

3. DESCRIPTION OF SENSOR (Fig. 1)

Transmitted RF signal is generated by combining a local oscillator (LO) signal, with a reference signal at the intermediate frequency (IF). The RF signal becomes pulsed at the RF gate which modulates it at the pulse repetition frequency (PRF). The RF pulses are amplified by the power amplifier, and pass through the circulator to the Σ port of the comparator. The antenna array comprises four radiators. The phase shifters in the array serve to steer the beams and a null in azimuth. The scheme, known in the art as monopulse, provides azimuth angle measurement relative to the antenna axis. Received sum (Σ) signal arrives through the circulator to a receiving channel which contains a low noise amplifier (LNA), a first down converter, an IF amplifier (IFA), and a second down converter (called also synchronous detector, or second detector). Received azimuth difference signal (Δ_{Az}) is fed to a second, identical receiving channel.

The output of the second down converter in each channel is bipolar video (or "Doppler"), since its LO port is fed from the reference oscillator at the IF. The bipolar video is sampled and transformed into digital format, and it undergoes in phase and quadrature (I&Q) fast Fourier Transform (FFT) processing. The FFT results in a matrix of n rows corresponding to n range gates, and m columns, corresponding to m Doppler filters, having a total of n x m range-Doppler cells, representing, each, a terrain element/cell.

The signal levels stored in the matrix are compared to a noise riding threshold (NRT). The NRT is based on measuring the noise level at transmission pauses, which take place periodically. During these pauses, the output of the FFT is the result of thermal noise, and possibly external sources of noise. Signals whose levels surpass the NRT are considered "legitimate", and are fed to the processor.

The processor calculates the azimuth of each cell by comparing the recorded power levels, received through the sum and difference channels, using the well known off axis angle estimation scheme [ref. 5]). In addition, a null in the antenna pattern is created and pointed at a symmetrical range-Doppler cell, which constitutes an ambiguity (4.2 below).

Elevation angle of each terrain cell is then calculated from its Doppler and azimuth (4.3 below). At this stage, range, azimuth and elevation of all terrain cells within the sensor's coverage are known, and the processor generates a 3D map or skyline contours , as well as special warnings for the display (and headsets), when required. It also interfaces with other on board systems (navigation equipment, air data computer, audio system etc.) to correctly process and position the 3D map or contours and the warnings, and deliver them to the aircraft's displays and head sets.

The sensor can use (share) one or more of the organic displays of the aircraft, such as a head down display (HDD), a head up display (HUD) or a helmet mounted display (HMD) - if so equipped. If there are no organic displays in the aircraft, a dedicated display for the

sensor can be installed. Otherwise, a display can be eliminated altogether, while warnings would be given to the crew orally.

REMARKS

a) In the description above, an off axis monopulse azimuth estimation is included. It should be noted that this is not the only usable angle measuring scheme. Other schemes, such as interferometry (4.2 below) are also usable. The choice of the scheme may be affected by antenna size and installation, component selection and other considerations.

b) The description does not include pulse compression (PC). PC can be used in order to reduce the peak power (meaning a better LPI feature) while maintaining good range resolution, and achieving better resistance against extraneous or jamming pulses.

d) The description does not include a Sensitivity Time Control (STC) feature [ref. 8]. Such feature may be desired in order to reduce the overall required dynamic range, and can be implemented using circuitry known in the art.

e) In the block diagram, and elsewhere in the description, FFT is mentioned as the Doppler spectral analysis tool. It should be noted that while FFT is an appropriate way to implement Doppler spectral analysis, other kinds of processing may also be used for that purpose.

f) Otherwise it should be understood that the architecture of the sensor, described above, represents just one way of implementing the required radar receiver/transmitter, and many other ways to implement it exist. Examples of different implementations include other arrangements for the generation of the RF and reference signals, and other schemes of generating the output transmitted pulse.

4. PRINCIPLES OF OPERATION.

4.1. Doppler processing

The Doppler shift of each terrain reflection element in an airborne radar is proportional to the cosine of α (Fig. 2), and is equal to:

$$f_d = (2v_g\cos\alpha)/\lambda \quad . \; . \; . \quad \text{(Eq. 1)}$$

where v_g is the ground velocity of the aircraft and λ is the wavelength. If the radar flies at a very low altitude over horizontal, flat terrain, then the Doppler filter bank created by the FFT process effectively divides the sector of terrain covered by the radar into many narrow sectors, where each Doppler filter represents two terrain sectors, symmetrically located about the line of flight (LOF, see appendix A), as illustrated by Fig. 3

This principle, known as Doppler beam sharpening (DBS [ref. 6]) is applicable not only to a horizontal plane, but to any plane containing the LOF, at any orientation, including the vertical plane. Therefore, α effectively defines a cone whose axis extends from the radar antenna along the LOF, as illustrated by Fig. 4. Any radar reflector on the surface of the cone has a Doppler shift which corresponds to α, as stated by Eq. 1 above.

In fact and as already suggested by Fig. 3, as the Doppler filter has a certain bandwidth Δf_d, radar reflectors which are detected through the specific Doppler filter will be located between the surfaces of two cones, having opening angles of $(2\alpha - \Delta\alpha)$ and $(2\alpha + \Delta\alpha)$, where $\Delta\alpha$ corresponds to Δf_d and the relation is is expressed by:

$$\Delta\alpha \cong -\lambda\Delta_{fd}/2v_g(\sin\alpha). \quad . \quad . \quad \text{(Eq. 2)}$$

(accuracy of the equation is degraded as sector becomes close to LOF)

Looking from the radar along the LOF, the cross section of the two cones are two coaxial circles which form a ring. The radar reflectors which were detected through the specific Doppler filter are located within this ring (Fig. 5).

The m Doppler filters resulting from the FFT process create a set of m contiguous coaxial rings, containing, each, reflectors of a different Doppler filter, and having, each, a different α, as illustrated by Fig. 6.

The rings intersect with range spheres (the 3D analog of range rings in 2D geometry), dividing the terrain in front of the aircraft into many range-Doppler (terrain) cells, defined, each, by its range and its Doppler.

As can be seen from Fig. 6, the rings become thicker as α becomes smaller, due to the dependence on sin α in Eq. (2) above. The inner circle represents Doppler filter # m, which covers the highest Doppler frequency range and the lowest α. The center of the inner circle (and all other rings), represents the LOF.

So far it was implied that α is known from the Doppler filter number, or the number of the corresponding ring. This means that there is an uncertainty in regard to the α of an object, as expressed by Eq. 2 above, and this uncertainty increases as the object is getting closer to the LOF (that is, as α gets smaller). The uncertainty can be reduced (and accuracy improved) by interpolation: consider an object whose Doppler lies within Doppler filter #k, as illustrated in Fig. 7. As the filters overlap, the object will be detected by both filter #k and filter # k+1. However, there will be a difference in the detected signal levels received through the two filters, because the object's Doppler is closer to the center of filter # k. From the ratio between the two signal levels, a more exact value of f_d and α can be found through interpolation, in much the same way as it is done in a DF process. In fact, a more elaborate process is required, because in many cases the object may be detected by filter # k-1 too. Here again, the process is similar to a DF process, in the case of a multibeam antenna (such as implemented with the Rotman lens or Butler matrix).

The Doppler interpolation process has been shown to improve Doppler resolution by a ratio of 8 [Ref. 14]. To have an idea of the angular accuracy that can be achieved near the LOF (where it is needed most but is most difficult to achieve), assume, as an example, an FFT process of 64 points (and therefore 64 Doppler filters). The Doppler which corresponds to the value of the ground velocity vector is set to fall in filter #63 (or #62), to allow interpolation near this velocity, meaning also near the LOF. The angle off the LOF, spanned by filter # 63 is about 10^0. If a resolution improvement ratio of only 6 is assumed here, then an accuracy of around 1.7^0 can be expected.

Furthermore, an additional improvement of accuracy can be gained by on going averaging of successive results of α, which are produced, each, after completion of each FFT cycle. This improvement takes place especially when the results have degraded

accuracy due to a low signal to noise ratio. (It should be pointed out that the interpolation and averaging processes must be done on recorded signals which belong to the same range gate).

A further improvement in estimating the position of a cell/object, has to do with its angular movement in relation to the LOF. Such movement is expected from all objects as the aircraft advances, except objects which are very close to the LOF or wires (4.7 below). The improvement can be achieved by employing track smoothing, such as provided by the Kalman filter [ref. 8].

As mentioned above, as α increases, the rings, and sectors on the ground become thinner, resulting in smaller radar cross section (RCS) of the terrain elements. Combined with a possible decrease in antenna gain in these angles, this effect means that more transmitted power is required for terrain which is away from the LOF, if the same range performance is to be maintained at these angles. One way of addressing this problem is to determine that reduced range performance at these angles is allowed, because the closing velocity to terrain elements at these angles is lower, and the time to possible impact into them is longer.

However, there is also a way to compensate for the reduced RCS. As sectors at these angles are narrower, they can be combined without becoming too wide, and without surpassing the width of sectors that are closer to the LOF. The combination of these sectors can be done by summing the values recorded from a number of adjacent filters (belonging to the same range gate). The summing is equivalent to the well known post detection integration (PDI) process, and will result in a processing gain which will depend mainly on the number of integrated values.

It should be noted that as the sector of interest in front of the aircraft does not extend to $\pm 90^0$ (it may typically extend to $\pm 20^0$) not all Doppler filters have to be implemented.

However, if detection of wires is desired, then the sector of interest is wider (4.7 below).

4.2. Azimuth angle processing.

The azimuth of each range-Doppler/terrain cell or obstacle is measured, according to one embodiment of the invention, using off axis monopulse angle estimation [ref. 5]. A common way to implement this scheme is to look at the ratio Δ/Σ of powers received in the difference and sum channels, for each terrain cell or obstacle, and the phase relationship between the two. The power ratio provides a measure of the angle, and the phase provides the sign (side in relation to the null of Δ). A look up table, relating power ratio and phase to angle can be prepared in advance and stored in the processor. Both power levels and phases of the two values are taken from the FFT results.

The intersections of two conical surfaces representing the frequency coverage of a Doppler filter with flat terrain, result, in most practical cases, in two hyperbolas. The intersections of two range spheres representing the coverage of a range gate with the same terrain, result in two circles. The intersections of the hyperbolas and the circles on the terrain, result in two symmetrical range-Doppler cells, which look like four sided polygons. Such hyperbolas, circles and range-Doppler cells on the terrain are illustrated in Fig. 8.

The half head angles of the cones (values of α) were 20^0 and 22^0. The radiuses of the range spheres were 235m and 250m. The flight altitude was 50m. The two range-Doppler cells are symmetrical about the LOF only when terrain is flat and horizontal, and LOF is horizontal. However, for the sake of description simplicity, we'll refer to one of the cells as the "cell of interest", and to the other as the "symmetrical cell".

To measure the azimuth of a cell, backscatter from the symmetrical cell should be eliminated from both of the received Σ and Δ signals used for the calculation. This can be done by directing a null in both Σ and Δ antenna patterns at the symmetrical cell. To do so, an appropriate phase shift has to be applied to the phase shifters connected to the antennas in the antenna assembly (Fig. 1 above). Fig. 9 shows a simulated radiation pattern of a usable monopulse antenna array, having sum and difference patterns, and a null common to both.

Horizontal axis shows azimuth in degrees. Vertical axis shows relative gain in dBs. The antenna is a linear array of four radiators (antennas), with a uniform spacing of 0.57λ among them. The radiation pattern of a single radiator was assumed to be a cosine function of θ. Weighting of a 0.5 factor (in voltage) was applied to the outer radiators, to bring about positioning of a common null in both Σ and Δ patterns. A uniform phase shift was applied between adjacent radiators to position the common null at at $\theta = -18^0$ (changing phase shift would move the null, but would keep it common to both Σ and Δ patterns). At the same time, this phase shift has moved the peak of Σ to about $+17^0$, allowing azimuth measurement in the region of 0 to $+15^0$.

The pointing angle of the null will be determined through simulation, so as to provide the best suppression of the symmetrical cell backscatter, where it is needed most. It can of course be changed by the sensor during flight, as necessary.

In any case, a residual signal from the symmetrical cell will always be present, and will usually cause an error in the azimuth measurement. This error can be estimated from Meade's formula [13]:

$$\text{Eq. 3} \ldots \quad \frac{\Delta\theta}{\theta_D} = \frac{a^2 + a\cos\xi}{1 + a^2 + 2a\cos\xi}$$

The formula allows estimation of the angular error $\Delta\theta$ in measuring the angle to a signal source, in the presence of another signal source having the same frequency. The parameters are the angular separation θ_D between two signal sources (the cell of interest and the symmetrical cell, in our case), the amplitude ratio (a) between the two signals (symmetrical over interest) and the phase difference ξ between the two signals.

The integral (or average) of $\Delta\theta$, when ξ changes from 0 to 2π is zero. Similarly, if results from a number of measurements, (each of them taken with a different, random value for ξ) are averaged, then the error tends to average out. It is expected that slight changes in geometry which take place among consecutive measurements will cause ξ to have different, random and uniformly distributed values, averaging out the error. A way to enhance changes in ξ between measurements is to change frequency between them, that is to use frequency diversity/agility. Depending on parameters, the process can be lengthy, since each measurement requires one FFT batch, which takes one integration period.

The time required for the process can be reduced, however, to one integration period, by performing the FFT processes of the different frequencies **in parallel.** This can conveniently be done thanks to the relatively long pulse repetition interval (PRI), which allows interleaving pulses of different frequencies, (being transmitted and received by the same transceiver).

The scheme can be clarified by the following example: Suppose velocity is 70m/sec (a little above 130kts), and wavelength is 7cm. Maximum Doppler is 2x70/0.07 = 2,000Hz. The required PRF is a little higher - say 2030Hz, so the PRI is 493μsec. The reqired PRI for an instrumented range of, say, 1,500m is only 10μsec. We can therefore interleave many pulses, having different frequencies, as shown in Fig. 10.

Pulses F1 and F2 are separated from each other by more than 10μsec (PRI required for instrumented range of 1,500m), so that by the time pulse F2 is to be transmitted, all the echoes of pulse F1 will have been received. The same is true for the separation between pulses F2 and F3, F3 and F4, and so on. If one wants to perform an FFT of, say, 128 points (pulses), than by the time 129 F1 pulses have been transmitted, 128 pulses of each of the other frequencies will have been transmitted too. Therefore, during that time (128 x 493μsec. = 63msec., in our example), one can perform in parallel the FFT processes for all frequencies. He will have after that time the detected results of all frequencies, ready for summation/averaging.

This scheme of frequency diversity/agility has two additional advantages, not directly related to the basic function of the sensor:

a) Frequency agility improves the sensor's resistance to enemy ECM, and makes it more difficult to detect by enemy ELINT/ESM (giving it a better LPI feature). Better ECM resistance and LPI features are desirable in military use.

b) Summation of FFT results from different frequencies, which is part of the averaging process, is equivalent to post detection integration, and therefore it improves probability of detection (Pd) for a given transmitted power, allowing to further reduce required transmitted power.

It should be noted that off-axis monopulse angle measurement as described above is not the only azimuth measuring scheme, usable for the invention. For example, here is a description of a scheme based on interferometry (Fig. 11).

Each pair of antennas forms, together with its connecting hybrid, an array. The receivers are connected to the **difference** outputs of the hybrids, so that every one of the two arrays (pairs) has a null in its pattern, and the nulls can be pointed to any direction within a certain sector, by changing the phase shifts. Alternatively, the nulls can be steered by phase shifts performed digitally, after FFT (not shown).

The scheme has now two receiving and processing channels, fed, each, by an antenna array. DF of the cell of interest is performed by phase comparison between its detected signals in the two channels.

Here again, the antenna arrays can be expanded to produce a steerable elevation null (see above).

4.3. Calculation of elevation/depression angle.

Once the azimuth angle of a terrain cell is known, its elevation/depression angle can be calculated, using its measured α. The geometry is described in Fig. 12, which contains also the three planar triangles used to derive the expressions.

O is the origin, where the radar is located. The LOF coincides with the negative direction of the x axis. A denotes the position of the terrain cell of interest, whose azimuth is θ and whose elevation/ depression is ϕ. R (OA) is the range to the terrain cell. Triangle ABC is a right triangle in a plane parallel to the zy plane.

From the planar triangles one can derive the following relations:

$$(OC) = R\cos\phi \quad . \; . \; \text{(Eq. 3)}$$

$$a = (OC)\sin\theta = (R\cos\phi)\sin\theta \quad . \; . \; \text{(Eq. 4)}$$

$$b = R\sin\phi \quad . \; . \; \text{(Eq. 5)}$$

$$c = R\sin\alpha \quad . \; . \; \text{(Eq. 6)}$$

For triangle ABC one can write:

$$a^2 + b^2 = c^2 \quad . \; . \; \text{(Eq. 7)}$$

Expressing a, b, c in terms of Eq. 4 through 6 above, and solving for cos ϕ yields the following expression:

$$\cos\phi = \frac{\cos\alpha}{\cos\theta} \qquad . \; . \; . \; . \; \text{(Eq. 8)}$$

This expression allows to calculate ϕ from α (related to the specific Doppler) and θ - the azimuth - obtained through the DF process. To eliminate the need for calculation, a two dimensional table, containing m' x k values can be prepared in advance from Eq. 8, where m' is the number of discrete values α can have, and k is the number of discrete values θ can have. The table will allow looking up the value of ϕ from any combination of α and θ.

The elevation angle calculation will still be valid during turns, when the aircraft is at a roll angle (bank), as long the azimuth angle is measured correctly.

4.4. Resolving elevation/depression angle ambiguity

Note that the calculation of ϕ is ambiguous in the sense that its value can be negative, signifying depression, and positive, signifying elevation. In other words, as any calculated

value of ϕ may mean either depression or elevation, both have to be displayed, so every terrain element or obstacle will have an image, and it may not be known which is the true element and which is the image.

This is of course an unacceptable ambiguity, because the crew has to know where is the terrain or obstacle, in order to maneuver and avoid them when necessary. Following is a discussion of the ways to resolve the ambiguity and maintain flight safety.

Fig. 13 is an example of a display showing a terrain contour below the LOF/flight plane (The flight plane (FP) is a plane determined by the LOF and a horizontal line perpendicular to it (App. A)), and the contour's image.

As terrain contour in this example is below the FP, its image is above it, and there is no overlap between them. In this case there is no doubt that terrain is below the FP, so the contour above the FP is declared "image" and is eliminated from the display. The LOF is also shown, with a safety circle around it. Its radius represents α_s - half head angle of a safety cone. In order to be safe, all terrain elements and obstacles have to be outside the circle. The value of α_s is dependent on range, and a number of safety circles with different radiuses may be displayed, for different ranges. In our case (Fig. 12 above) the safety circle is free of any terrain or obstacles, and an avoidance maneuver is not required.

Fig. 14 shows another case, where terrain contour is close enough to the LOF/FP, part of it is higher than LOF/FP and part of it is within the safety circle.

This is of course a situation that requires a safety maneuver, since part of the terrain contour is within the safety circle. The required maneuver is a pull up, possibly combined with a turn. The pull up maneuver has to continue until the LOF/FP rises above the terrain contour, overlap condition ceases and the upper contour can be declared image and eliminated from the display, as before (Fig. 12). The maneuver may have to continue further, until the terrain contour completely clears the safety circle.

In case of a point obstacle, which protrudes above the contour and penetrates the safety circle or causes overlap, the procedure is similar.

In case of a horizontal wire (possibly when the sensor includes also hardware and features for wire detection, 4.7 below) the situation and solution are different.

If the wire is below FP (and image above it), a pull up maneuver will cause the wire display to move down relative to the FP. The image display will move up (to maintain symmetry about the FP). The system will sense the increase in separation between wire and image displays, declare the upper display "image" and eliminate it from the display.

If the wire is actually **above** the FP and image is below it, then a pull up will cause the wire display to move **down** towards FP, while image display will move **up** towards FP.

In this case the system will sense that the separation decreases, declare the lower display "image" and eliminate it from the display.

Similarly, a push down maneuver can also be used to resolve the ambiguity. In this case, if the wire is below the FP, wire and image displays will get closer, and if wire is above the FP, wire and image displays will further separate from each other.

A variation of the wire case is the slanted wire. In this case there will be an image, which, unlike the former cases, will not be a mirror picture of the true display.

However, image resolution in the case of the slanted wire is the same as for the horizontal wire above, using a pull-up (or a push-down) maneuver.

There is a way to eliminate the need to maneuver in order to resolve the ambiguity in all of the above cases. The result of the elevation/depression calculation (4.3 above) is the angle ϕ, and the correct position of the object can be ϕ below FP **or** ϕ above it. To find out which of these possibilities is the true one, a null in the elevation antenna pattern can be pointed at the lower angle (ϕ below FP). If a decrease in detected echo power is sensed,

then the lower angle is the true object position and the higher angle points at the image. If no decrease is sensed, then the object is at the higher angle (ϕ above FP), and the lower angle (ϕ below FP) points at the image (in a similar way, ambiguity can be resolved by pointing the null at the high angle).

The required elevation null can be created by replacing each radiating element in the antenna of Fig. 1 above, by two elements, arranged one above the other, as illustrated in Fig. 15.

Antenna radiators are shown as squares. Each of the original radiators in fig. 1 above is now replaced by an assembly which contains two radiators, connected to a hybrid through phase shifters. The difference output of the hybrid is used, and the assembly produces a null, that can be pointed at any elevation within a known elevation sector, by appropriately adjusting the phase shifters (one of the phase shifters in each assembly can be eliminated by replacing it with a fixed phase shift). The principle of generating and pointing the null is similar to the one described for the azimuth null (4.2 above).

Note that the ambiguity resolution procedure for a wire can be done separately from the resolution of ambiguity for terrain and point obstacles (as described above in this section), and in parallel to it.

4.5. Ground reflection from obstacles (specular reflection is addressed).

Elevation angle measurement accuracy is often degraded by the presence of a ground reflection of the target's echo (multipath effect, Ref. 11). This effect takes place when the antenna radiation pattern in the vertical plane is wide enough to "see" the reflection point (and this is usually true in the case of the present invention). It should be noted that the ground reflection is an entirely different effect than the elevation ambiguity discussed in 4.4 above. Each of these effects can be addressed separately, and if possible, in parallel.

Fig. 16 illustrates the geometry of specular reflection in a typical case.

Assume for simplicity that the azimuth of the object's tip, θ, is zero. It can be shown that the Doppler shift of the object's tip echo can be expressed as:

$$f_{do}(t) = -\frac{2}{\lambda}\cdot\frac{d}{dt}\left[\sqrt{(r_o - v_g\cdot t)^2 + (h_r - h_o)^2}\right]$$

and the Doppler shift of the tip's reflection image can be expressed as:

$$f_{di}(t) = \frac{f_{do}(t)}{2} - \frac{1}{\lambda} \cdot \frac{d}{dt}\left[\sqrt{(r_o - v_g \cdot t)^2 + (h_r + h_o)^2}\right]$$

where:

- r_o is the horizontal range to object's tip
- h_r is aircraft's altitude
- h_o is object tip's height

(the expression is valid and identical when $h_r > h_o$ or when $h_r < h_o$)

The object's tip and it's reflection image elevation angles, β and γ (respectively) are related to these Doppler shifts by Eq. 1 above. These angles, as deduced by the sensor from Doppler measurements, are plotted in fig. 17, for the following set of parameters:

- $r_0 = 1{,}000$m
- $h_r = 50$m
- $h_o = 25$m
- $v_g = 70$m/sec.

Horizontal axis shows time in seconds. Vertical axis shows elevation angle in degrees. At t = 0, range is 1,000m, and object overpass is at 14.3sec.

And $|\gamma|$ is always greater than $|\beta|$. Depending on the width of the Doppler filter and the other parameters, signals related to these angles can fall in separate filters or within one filter.

In the first case (β and γ in separate filters), measured value of β is unaffected by the ground reflection.

In the second case (both in same filter, typically at a longer range and/or lower altitude), as the sensor performs interpolation (4.3 above), the resulting Doppler is shifted down by the multipath reflection. This shift down in the measured Doppler translates into a larger measured depression.

Ways to correct the measurement are:

a) Assume presence of a reflection image. Estimate through simulation a fixed value for its effect on elevation/depression. Correct β up according to the estimate. The correction will be inaccurate, but will result in presenting a **higher** obstacle, possibly requiring a more strict avoidance maneuver, so that flight safety is not jeopardized by the inaccuracy.

b) Try to separate between the two signals, in a way analog to the separation of two targets in azimuth in a scanning radar, based on the resulting antenna pattern recorded from the intensity of the reflected echoes [Ref. 10]. Here, the scanning movement of the antenna has to be replaced by moving, in frequency, of the Doppler filter bank. This can be done by changing the frequency of the reference oscillator (Fig. 1).

c) search with a notch (As described in 4.4 above) below measured value of β, for a point where measured β changes **up**, indicating that the reflected image has been attenuated by the null.

Besides the ways described above to reduce the effect of ground reflection, it should be pointed out that the ground reflection can be weakened in the elevation sector around the Brewster angle by the use of vertical polarization [11]. Therefore, vertical polarization should generally be preferred over horizontal polarization, except for the case of wire detection (4.7 below).

4.6. An alternative elevation/depression angle measurement scheme.

In a different embodiment of the invention, elevation angle ϕ of each range-Doppler cell is measured by a conventional DF scheme, while azimuth angle θ of the cell is computed from α and elevation angle ϕ, using eq. 8 above.

In this case there is no elevation ambiguity, but multipath ground reflection is expected and has to be suppressed, preferably by pointing a null to it. At the same time, an azimuth null has to be pointed at the symmetrical cell which exists here as before (Fig. 8 above). This null will also serve to resolve the azimuth ambiguity resulting in this case from Eq. 8. The scheme can be identical to the one illustrated in Fig. 15, except that the array has to be rotated 90^0 (to have two columns of 4 radiators each). Elevation will be measured using the off axis monopulse scheme, the ground reflection will be suppressed by the common null (Fig. 9 above), and the symmetrical cell signal will be suppressed by the null used earlier to attenuate the elevation image.

A residual multipath reflection, present after pointing a null to the reflecting point, can be averaged out it out through frequency diversity/agility [Ref. 12], as described in 4.2 above.

It should be noted that off axis monopulse estimation is not the only usable elevation measuring scheme. Here again (as in 4.2 above), another scheme, such as interferometry can be used.

4.7. Wire detection and recognition.

The current invention, as described heretofore, has a partial capability to detect and recognize suspended wires, as such. A wire reflects back electromagnetic energy from the point of normal impinging (the point on the wire - assumed here to be a strait line - at which a normal to the wire meets it, Fig. 18). This reflection would look to the computer like a point obstacle, and thus will not convey the true nature of a wire, which usually extends both ways from the impinging point, and constitutes a hazard also outside this point.

Wires can be recognized by the sensor, however, based on three special attributes they have, which are usually not possessed by point obstacles:

a) Wires may be high enough, so as to look suspended. In other words, a wire may appear at a certain elevation, while just below it (at the same range and azimuth) there is no reflection.

b) The reflection point from a straight wire at low elevation will always appear at a fixed azimuth and have fixed closing rate (radial velocity) as long as the aircraft advances

in a straight line. This is not the case with point obstacles, which, unless very close to the LOF, will move in azimuth and change closing rate as the aircraft advances.

c) Wires are suspended from pylons, which are regularly separated from each other. If such a regular arrangement of point obstacles is found by the sensor, the presence of pylons can be suspected, and virtual wires can be drawn among them and displayed, with a proper warning of suspected wires.

If a wire is declared or suspected using the above criteria, it may also assumed to be horizontal, as is most likely (unless in a mountainous area). If this is the assumption, then the orientation of the wire in the horizontal plane can be calculated from the azimuth of the reflecting point, to which the wire is perpendicular. The wire can be displayed as such, with its orientation, on a PPI (plan position indicator), which provides a look of the aircraft and the terrain from above.

A more decisive way to detect and recognize wires, is to use the method of US patent 6,278,409 (Zuta), where wires are detected and discriminated from other objects using a polarimetric radar. If the RF is low enough (say, in L band, Ref. 15), the RCS of a wire is high in normal impinging, when the wave polarization is parallel to the wire. However, when wave polarization is perpendicular to the wire, the RCS is low. If the backscatter from a range-Doppler cell is strong in one polarization and weak in the orthogonal polarization, then the range-Doppler cell in question is likely to contains a reflection point of a wire, and the wire is parallel to the polarization which produced the strong backscatter.

If only horizontal wires are to be detected and recognized, the sensor can switch between horizontal and vertical polarizations, or use both in parallel. If detected backscatter is considerably stronger in horizontal polarization than it is in vertical polarization, then it is likely that a horizontal wire (or a group of parallel wires) have been detected.

If slanted wires are also to be detected and recognized, than polarization has to be rotated - continuously or in steps (see below). In this case, backscatter received at any time is being compared continuously to backscatter received at the orthogonal polarization (measured earlier, later or at the same time). When a pair of two orthogonal polarizations is found, in which one backscatter was strong compared to the other, then a wire is likely to be present, and the wire is parallel to the wave polarization (orientation of the electric field) which produced the stronger backscatter. If the reflection point is not at a very high elevation, this orientation would also be the angle between the wire and a horizontal plane. As a clarifying example, assume that such pair of orthogonal polarizations - one oriented 30^0 from the horizontal and the other oriented 120^0, was found, and the stronger backscatter was received in the 30^0 polarization. The meaning is that there is a slanted wire and it is oriented 30^0 from the horizontal.

Measuring the azimuth to the reflecting point will complete the knowledge of the wire's orientation in space, and allow to display it in a useful manner.

If the reflection point is higher, then the polarization, as well as both azimuth and elevation of the reflection point would be required to determine the wire's orientation in space.

Polarization rotation may be required also when only horizontal wires are to be detected (see above), if the capability to detect and recognize wires has to be maintained

when the aircraft has a roll angle (bank, during turns, for example). In this condition, polarizations have to be stabilized by polarization rotation.

The spatial coverage (field of regard) of the wire detection function has to be around 180^0, since the aircraft can converge to a wire which is almost parallel to the LOF, and collide with it. In this case, the reflection point on the wire, close to 90^0 off the LOF, has to be detected.

Though antenna polarization rotation can be implemented mechanically, it may be desirable to implement it electronically, using dual polarization radiators, phase shifters and attenuators, as known in the art. Fig. 19 shows such an implementation in a radiator - one of a number that can form an array, capable of polarization rotation.

The square represents a dual polarization radiation element, such as a microstrip (patch) antenna, fed by two signals through two points. The signal (in transmission) is divided to two channels by a hybrid. The phase shifter has to switch between 0^0 and 180^0. The attenuators have to be capable of continuous or stepped change of attenuation. The scheme provides a continuous or stepped change of polarization over 180^0 (practically the same as 360^0).

As mentioned above in this section, recognition of wires through polarization rotation requires a relatively low frequency. On the other hand, terrain and obstacle mapping can (but does not have to) use a higher frequency, which will reduce FFT processing time and allow a higher rate of information. It is conceivable that the sensor will contain two transceivers for the two functions, or just one for the two.

5. GENERATING THE DISPLAYS AND WARNINGS

5.1. Generating the 3D terrain and obstacle map, with special warnings

Based on the coordinates R, θ, and ϕ, obtained so far for each terrain element or obstacle, a 3D map can be readily generated. Point obstacles like pylons will also appear on the map. If big enough, these may extend over more than one cell on the map. These obstacles will have usually specific reflection intensities, related to their specific RCS values, usually different from their surrounding terrain. The obstacles will be distinguishable to the computer, and if their intensity will be expressed in the map, then they will be detectable to the eye, due to their contrast. As the angular distance of any cell from the LOF (α) is known, a special warning can be displayed, accompanied by an aural signal, to notify the crew of a condition where the α of a specific cell or obstacle or group of cells/obstacles is smaller then a predetermined (or adapting) safety value. If actual impact (zero α) is predicted, a more severe warning can be given, along with an indication of the time to impact (TTI).

5.2. Generating terrain contours.

A different kind of display which can be generated from the 3D data is a contour (sky line) display, which may possibly be easier for the crew to interpret. An example of such a display is brought in Fig. 20.

The lower trace is the contour at a relatively short range, such as 200m (600'). The middle trace is the contour at a middle range, such as 500m (1,500'), and the upper trace is the contour at a longer range, such 1,000m (3,000'). The crew can assess the angular displacement of the LOF symbol from the contours and maintain adequate clearance from them, with the aid of the safety circle. It should be noted that the radius of the safety circle (which represents a safety value for α) may be related to range. As an example, in order to keep a fixed clearance from a terrain cell or obstacle along the flight path, a bigger radius is required at a short range, and a smaller radius is required at a long range.

As in 5.1 above, special alarms can be presented on the contour display and sounded in the headsets.

It should be noted that these display concepts are but samples from a large variety of possibilities, and that the styles of display can be shaped at will to the requirements.

6. A SIMPLIFIED SENSOR AND DISPLAY

A significant simplification and saving in hardware and software can be implemented by using a single radiator antenna, and eliminating any DF and nulling. Doppler processing is done as described in 4.1 above, resulting in a division of the space in front of the aircraft into range-Doppler cells. Azimuth and elevation of terrain cells or obstacles are not known to the sensor and cannot be displayed in this embodiment. However, range and angular displacement from the LOF, α, are known. Conditions in which the angular displacement of a cell/object is smaller than the safety margin are sensed and displayed, and additional special warnings can be generated.

An example of a possible display format for this embodiment is shown in Fig. 21.

Displayed are safety circles for three ranges (dotted). Displayed also are terrain contours (solid) for corresponding ranges, which are deformed and appear as half circles. As long as a terrain contour for a certain range is outside the corresponding safety circle, situation is safe. If a contour has contracted and entered its corresponding (associated to the same range) safety circle, it is not known where (in which side) is the obstacle or terrain feature that caused this situation, but a strait pull up maneuver would cause the aircraft to get out of the situation.

If desired, a crude indication of the side (left or right) of a large obstacle which is close to the LOF can be provided with a relatively minor complication. This capability would require the use of two channels, comprising, each, an antenna and a transmit/receive channel. The two antennas will be squinted out from each other in a horizontal plane, such that one is looking a little to the right of the aircraft's longitudinal axis, and the other a little to the left of it, with a common sector. Comparison between signal strengths of the same range-Doppler cells in the two channels, will provide the left/right indication.

The same can be achieved also with a single channel, switching between the two antennas (or a two radiator antenna array whose lobe can be switched between the two azimuth positions). This scheme will require at least two FFT periods to provide the indication, whereas the two channel scheme can use a single FFT period. The choice between one channel and two channels may be affected by this difference, and would be related also to the choice of RF. For example, if a wire detection sensor is to be combined,

and if the same channel/s are to be used for both TA and wire detection, then low frequency is to be used (see app. B). In such a case, maximum Doppler is lower and the FFT process takes longer, so a two channel configuration, requiring a single FFT period is preferable, in order to maintain an adequate rate of information renewal.

It is also conceivable that the simplified embodiment be used as a **mode** in one of the other embodiments described above, in case of loss of the LOF information (App. A below), or due to another malfunction which may warrant this mode. The mode may also be used in cases where a newly detected object constitutes a collision hazard, because it is close enough to the LOF, and at a short range. Upon detection (after one FFT period) the sensor will display the situation in the simplified mode, and then revert to normal mode after azimuth and elevation will have been measured (possibly taking a few more FFT periods).

APPENDIX A: DEFINITIONS OF LINE OF FLIGHT (LOF) AND FLIGHT PLANE (FP)

1. The Line of Flight (LOF) is a line which coincides with the velocity vector of the aircraft. The aircraft's longitudinal axis (ALA), on the other hand, is a geometrical line that can be rigidly defined for the aircraft's fuselage. As illustrated in Fig. 22 , LOF and ALA do not necessarily coincide.

The angular displacement between the two is dependent on flying conditions. As an example, in the final stage of landing, the ALA may point above the horizon, while the LOF points below the horizon.

A horizontal plane view of ALA and LOF will show that they do not necessarily coincide in the horizontal plane either, again, depending on flight conditions. The most common cause for a sustained difference between the two in the horizontal plane is side wind, which causes the aircraft to drift aside.

While the ALA is rigidly tied to the airframe and its orientation can be supplied by horizontal and directional gyros (used for instrument flying), LOF requires more elaborate calculation. It can be supplied, fully or partially from the aircraft's (or sensor's own) navigation (NAV) system.

The main reason to require knowledge of the LOF is the fact that azimuth is measured (4.2 above) relative to the antenna array structure, which is rigidly connected to the airframe and the ALA, while α is measuerd relativ e to the LOF. Calculation of elevation from azimuth, has to be done based on azimuth in respect to the LOF, so azimuth measured relative to the ALA has to be translated to azimuth in relation to LOF, through knowledge of LOF. When azimuth is calculated from elevation (4.6 above) , knowledge of LOF is needed to point the azimuth null. LOF is not required, however, for the simplified sensor (sec. 6 above). In case LOF becomes unavailable for any reason, the sensor has to resort to the simplified mode.

Another reason to require the LOF is the desire to center the display so that the crew will see the displayed objects at a direction which will allow them to easily look for them and find them outside.

2. The flight plane (FP) is a plane determined by the LOF and a horizontal line perpendicular to it.

APPENDIX B: LIST OF ABBREVIATIONS

3D	Three Dimentional
ALA	Aircraft's Longitudinal Axis
CFAR	Constant False Alarm Rate
CFIT	Conrolled Flight into terrain
COSRO	Conical Scan on Receive Only
DBS	Doppler Beam Sharpening
DF	Direction Finding

ECM	Electronic Countermeasures
EGPWS	Enhanced Ground Proximity Warning System
ELINT	Electronic Intelligence
ESM	Electronic Support Measures
FFT	Fast Fourier Transform
FP	Flight Plane
GPS	Global Positioning System
HDD	Head Down Display
HMD	Helmet Mounted Display
HUD	Head Up Display
I	In phase
I&Q	In phase & Quadrature (processing)
IF	Intermediate Frequency
IFA	Intermediate Frequency Amplifier
Kts	Knots
LBSORO	Lobe Switching on Receive Only
LO	Local Oscillator
LOF	Line of Flight
LNA	Low Noise Amplifier
LPI	Low Probability of Intercept
MEDEVAC	Medical Evacuation
MMW	Millimeter Waves
NAV	Navigation
NRT	Noise Riding Threshold
OA	Obstacle Avoidance
OASYS	Obstacle Avoidance System
PC	Pulse Compression
Pd	Probability of Detection
PDI	Post Detection Integration
PRF	Pulse Repetition Frequency
Q	Quadrature
RCS	Radar Cross Section
S&R	Search and Rescue
SDLVA	Successive Detection Log Video Amplifier

TA	Terrain Avoidance
TTI	Time to Impact

APPENDIX C: LIST OF SYMBOLS

English:

a	amplitude ratio of two signals
f_d	Doppler shift (Hz/sec.)
f_{dr}	Doppler shift of reflection
f_{do}	Doppler shift of object echo
h_o	height of object above ground, or object's tip height
h_r	aircraft's altitude
m	number of Doppler filters
m'	number of discrete values α can have
n	number of range gates
R	range to terrain cell
r_0	horizontal range to object or to object's tip
v_g	aircraft's ground velocity (m/sec.)

Greek:

α	angle between direction to a radar reflector (terrain element, obstacle etc.) and the LOF
α_s	half head angle of a safety cone
β	elevation angle of object's tip
γ	elevation angle of object tip's reflection image
ϕ	elevation/depression angle of terrain cell
θ	azimuth angle of terrain cell
θ_D	angular separation between two signal sources
ξ	phase difference between two signals

Δ difference antenna pattern (in a monopulse antenna); Power received through this channel

$\Delta\alpha$ angular width of cone surface

$\Delta\theta$ error in angle measurement

Δf_d bandwidth of Doppler filter (Hz)

λ operating wavelength of radar (m)

Σ sum antenna pattern (in a monopulse antenna); Power received through this channel

REFERENCES

1. US patent 5,465,142 (Krumes)
2. US patent 4,902,126 (Koechner)
3. Russian patent RU 2128846 (Kurilkin & Samarin)
4. US patent 5,847,673 (DeBell)
5. Barton: Modern Radar System Analysis, 1988, p. 421
6. Stimson: Introduction to Airborne Radar, 1983 edition, p. 561
7. Skolnik: Introduction to radar systems, third edition, 2001, "Second Generation MTD" p. 146
8. Skolnik: Introduction to radar systems, third edition, 2001, p. 261
9. Barton: Modern Radar System Analysis, 1988, sec. 11.2
10. Skolnik: Introduction to radar systems, third edition, 2001, p. 147 (bottom)
11. Barton: Modern Radar System Analysis, 1988, sec. 6.2
12. Barton: Modern Radar System Analysis, 1988, p. 529
13. Locke: Guidance, "Target Considerations", 1955, p. 440
14. US patent 6,278,409 (Zuta)
15. Kerr: Propagation of Short Radio Waves, MIT Radiation Laboratory series, Vol.13, 1951, sec. 6.

CLAIMS

1. General

1. A radar apparatus for 3D terrain mapping and obstacle detection for helicopters and other aircraft, having a broad, non scanning antenna beam, operating at a moderate radar frequency (L to X bands), comprising a transceiver with means for DF in azimuth or elevation and circuitry for Doppler spectral analysis. When azimuth is measured through DF, elevation angle of each range-Doppler cell is calculated from azimuth and Doppler, and when elevation is measured through DF, azimuth angle is calculated from elevation and Doppler.

2. Display and warnings

2. An apparatus as in claim 1, where based on the three coordinates obtained for each cell, a 3D terrain map or sky-line contours are generated for display, along with safety circles. A number of contours and safety circles can be presented, for a number of ranges. Additional, special warnings can be added on the display and in the headsets.

3. Doppler interpolation

3. An apparatus as in claims 1-2, where Doppler measurement is further refined by interpolation and maximum expected Doppler is set to fall in a Doppler filter which is close to, but not identical with the last filter, this last filter corresponding to the maximum instrumented Doppler.

4. Doppler averaging

4. An apparatus as in claims 1-3, where Doppler measurement is further refined by averaging of consecutive FFT results.

5. Doppler track smoothing

5. An apparatus as in claims 1-4, where Doppler measurement is further refined by track smoothing, such as the Kalman filter.

6. Summation of adjacent filters

6. An apparatus as in claims 1-5, where results from a number of adjacent Doppler filters, corresponding to backscatter from a sector away from the aircraft's velocity vector, are summed to improve signal to noise ratio.

7. Partial filter implementation

7. An apparatus as in claims 1-6, where only part of the Doppler filters, related to the sector of interest in the front of the aircraft are implemented.

8. Off axis monopulse

8. An apparatus as in claims 1-7, where azimuth of a terrain cell is measured through off axis monopulse azimuth estimation.

9. Suppression by common null

9. An apparatus as in claim 8, where a radar return from a terrain cell belonging to the same range-Doppler cell of interest and located on the opposite side of the aircraft's velocity vector is suppressed by a null, common to both sum and difference patterns.

10. interferometry in azimuth
An apparatus as in claims 1-7, where azimuth of a terrain cell is measured by interferometry, and where a radar return from a terrain cell belonging to the same range-doppler cell of interest and located on the opposite side of the aircraft's velocity vector is suppressed by a null.

11. Averaging out residue
11. An apparatus as in claim 1-10, where a radar return from a terrain cell belonging to the same range-Doppler cell of interest and located on the opposite side of the aircraft's velocity vector is suppressed by a null, and where the error resulting from a residue of the suppressed return is averaged out when summing/averaging a number of measurements, using a single frequency or frequency diversity/agility.

12. parallel FFT processes to average out residue
An apparatus as in claims 10-11, where a number of azimuth measurements is done through spectral analysis processes done in parallel, interleaving pulses of different frequencies.

13. Track smoothing in azimuth measurement
An apparatus as in claims 1-12 where azimuth measurement is further refined trough track smoothing, such as the kalman filter.

14. A 4 element array
An apparatus as in claim 1-9, 11-13, using a four element array, each element being connected through a phase shifter, and arranged as an azimuth monopulse antenna, having steerable sum and difference lobes and a steerable null, common to both sum and difference lobes

15. An 8 element array
An apparatus as in claims 1-14, using an array of 8 elements, arranged in two rows situated one above the other, capable also of generating a steerable null in elevation.

16. Ambiguity resolution, no intersection
An apparatus as in claims 1-15, having an elevation ambiguity resolution scheme which declares the upper horizon contour an image and eliminates it from the display - provided that the true contour and its image do not intersect.

17. Ambiguity resolution, intersection - pull up
An apparatus as in claim 1-15, having an elevation ambiguity resolution scheme, based on a pull up maneuver, in case the true contour and its image do intersect. The maneuver separates the contours, bringing them to the condition where they are resolved as in claim 16

18. Ambiguity resolution by null
An apparatus as in claims 1-15, where ambiguity resolution between object (terrain cell or obstacle) and image displays is done by pointing a null in the elevation pattern of the antenna to either or both elevations. When the null is pointed at the object's actual elevation, a decrease of object backscattered power will be sensed.

19. Multipath suppression by filter separation
An apparatus as in claims 1-18, where mutipath reflection is separated from actual object backscatter and eliminated from the display, based on the difference in Doppler between the two, the two being in two separate Doppler filters.

20. Multipath correction by fixed bias
An apparatus as in claims 1-18, where effect of multipath reflection on object's elevation/depression received in the same Doppler filter as the actual object's backscatter, is corrected using a fixed bias.

21. Multipath separation as in beam
An apparatus as in claims 1-18, where multipath reflection received in the same Doppler filter as the actual object, is separated from the object in a way analog to the separation of two targets which are received within the same beamwidth in a scanning radar.

22. Multipath suppression by null
An apparatus as in claims 1-18, where multipath reflection received in the same Doppler filter as the actual object is suppressed by pointing a null in the antenna pattern to it.

23. Off axis monopulse elevation measurement
An apparatus as in claims 1-7, where off axis monopulse estimation is used to measure elevation, and azimuth is calculated from elevation and Doppler, and where multipath reflection is suppressed by the null common to the sum and elevation difference lobes, and radar return from a terrain cell belonging to the same range-Doppler cell of interest and located on the opposite side of the aircraft's velocity vector is suppressed by a null in azimuth, using the array antenna described in claim 15, rotated 90^0.

24. Elevation measurement, suppression of residuals in elevation
An apparatus as in claims 23, where a residual of the multipath reflection is averaged out through averaging a number of measurements, using a single frequency or frequency diversity/agility.
25. Elevation measurement, regular monopulse, parallel processing
An apparatus as in claim 24, where averaging with frequency diversity/agility is implemented in parallel, by performing spectral analysis processes in parallel, interleaving pulses of different frequencies.

26. Interferometry in elevation
An apparatus as in claims 1-7, where elevation is measured though interferometry, where multipath reflection and radar return from a terrain cell belonging to the same range-Doppler cell of interest and located on the opposite side of the aircraft's velocity vector are suppressed by nulls in azimuth and elevation.

27. Interferometry in elevation with 8 element antenna
An apparatus as in claim 26, using an array antenna having 8 elements, arranged in two columns, each fed by a phase shifter, this array being capable of generating steeranle nuls in both azimuth and elevation.

28. Simplified sensor
An apparatus or mode where spectral analysis is done as in claim 1, determining the Doppler of the object nearest to the aircraft's velocity vector at a certain range, and displaying a distorted contour in the form of a half circle around the aircraft's velocity vector, whose radius represents the angular distance of this object from the aircraft's velocity vector.

29. Simplified display, a number of contours and safety circles
An apparatus as in claim 28, where a number of distorted contours are displayed, for a number of ranges, along with a number of safety circles.

30. Simplifid display, a number of contors, coarse DF
An apparatus as in claim 29, where coarse azimuth DF is performed, providing an indication of the side in which a massive object is situated

31. Wire detection, no polarimetry, fixed azimuth
An apparatus as in claim 1, providing also detection of suspended wires, based on normal impinging, where discriminating wires from other objects, is based on the fact that the reflecting point on the wire seems at constant azimuth as the aircraft advances, and the closing velocity to the point is constant.

32. Wire detection, discontinuity
An apparatus as in claim 31, where discriminating wires from other objects, is based on a discontinuity of backscatter in the elevation angle, when no backscatter comes from elevations between the wire and the ground.

33. Wire detection, arrangement of pylons
An apparatus as in claim 31, where wire is suspected based on detection of a regular spacing between point obstacles, indicating that these obstacles may be pylons, carrying wires.

34. Orientation, horizontal wire
An apparatus as in claim 31, where orientation of a wire in a horizontal plane is determined by taking the normal to the line of sight of the wire reflection point.

35. Horizontal wire, polarimetry
An apparatus as in claims 31-34, further including methods and hardware from US patent 6,278,409B1, where a fixed horizontal polarization and a fixed vertical polarization are used, and where the ratio of received backscatter intensities in the two polarizations are used to determine whether a horizontal wire is present.

36. Slanted wire, polarimetry, orientation
An apparatus as in claim 35, where polarization can also be rotated and where backscatter intensities measured at one polarization and at a polarization orthogonal to it are compared to find out if the ratio between these intensities is above a certain threshold, indicating the presence of a wire, whose orientation in space is parallel to the polarization which resulted in the higher backscatter intensity.

37. Horizontal wire, pol stabilization
An apparatus as in claim 35, where polarization rotation is used to stabilize orientation of the two orthogonal polarizations, when the aircraft changes its roll angle.

38. Wire ambiguity resolution, pull up
An apparatus as in claims 31-37, where ambiguity resolution between a wire display and its elevation image is based on a pull up maneuver, causing the wire display and its image to further separate from each other, if the wire is actually below the flight plane, and causing the wire display and image to get closer to each other, if the wire is actually above the flight plane.

39. Wire ambiguity resolution, push down
An apparatus as in claim 38, where the ambiguity resolution is similarly based on a push down maneuver.

40. Wire ambiguity resolution, null
An apparatus as in claims 31-39, where ambiguity resolution between wire and image displays and/or suppression of multipath reflections are done by pointing a null in the elevation pattern of the antenna to the elevation of either of the displays (true or image) or to the multipath reflection point.

For the applicant:

Fenster & Company, Patent Attorneys, Ltd
C: 357/02921

FIGURES

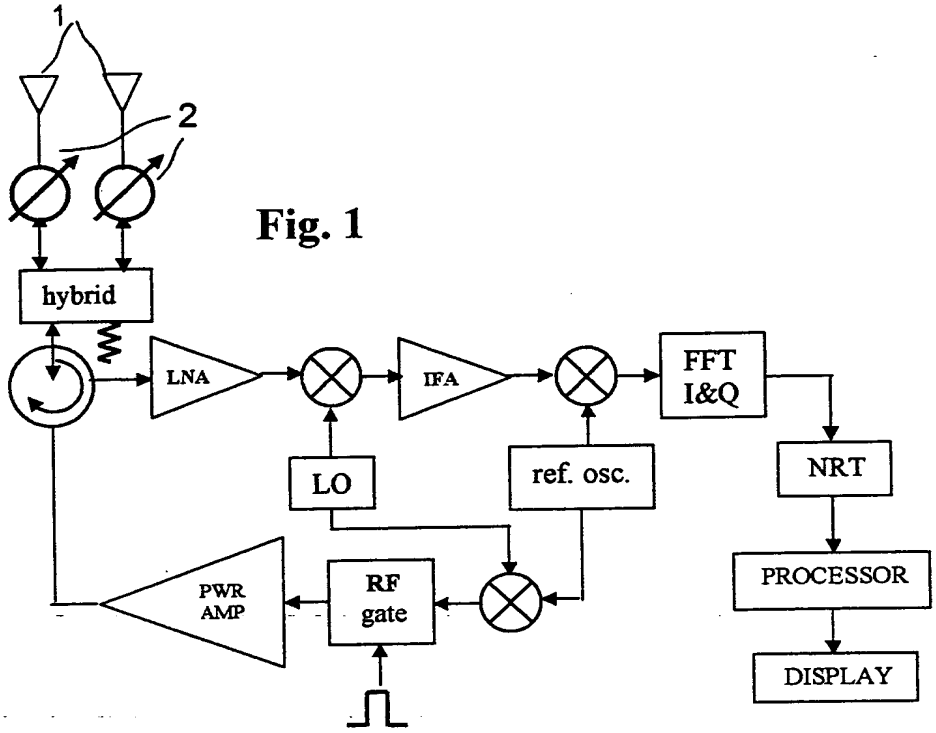

Fig. 1

1 Antenna assembly
2 Phase shifters

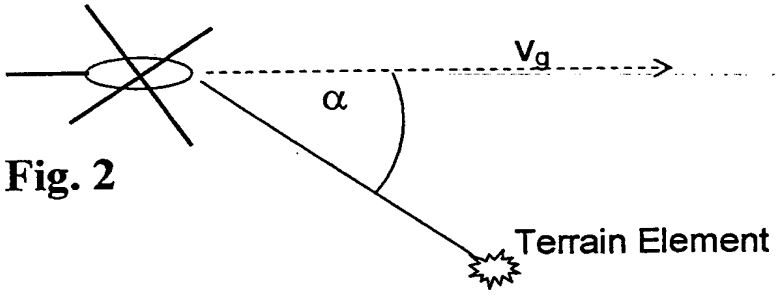

Fig. 2

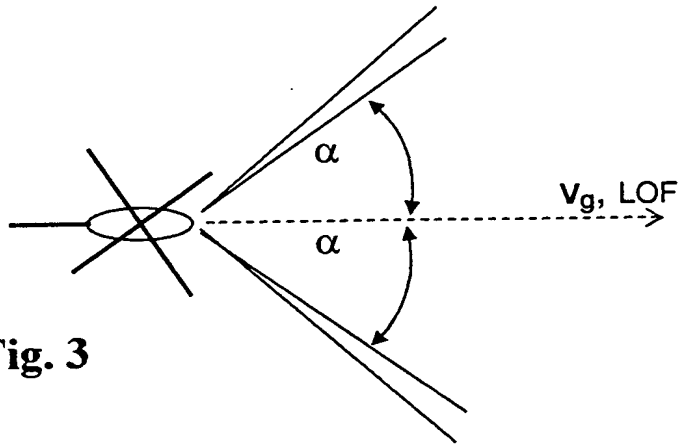

Fig. 3

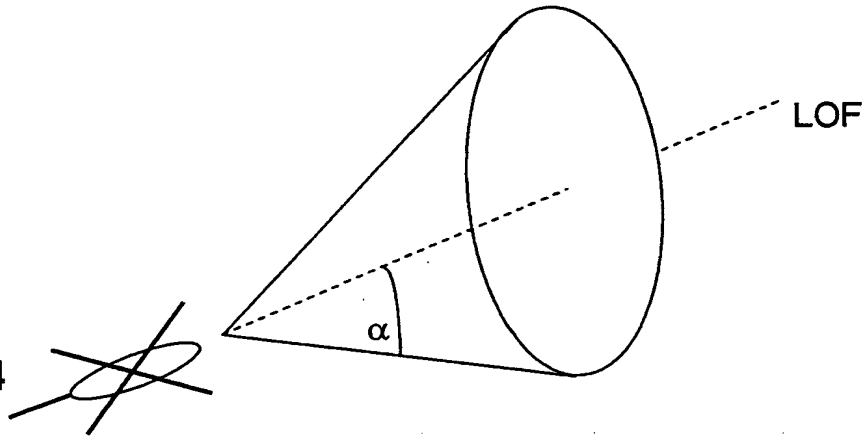

Fig. 4

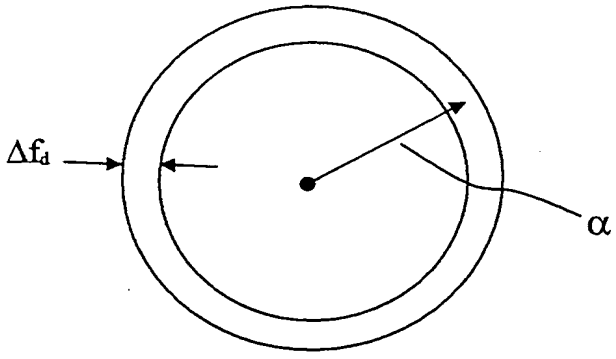

Fig.5

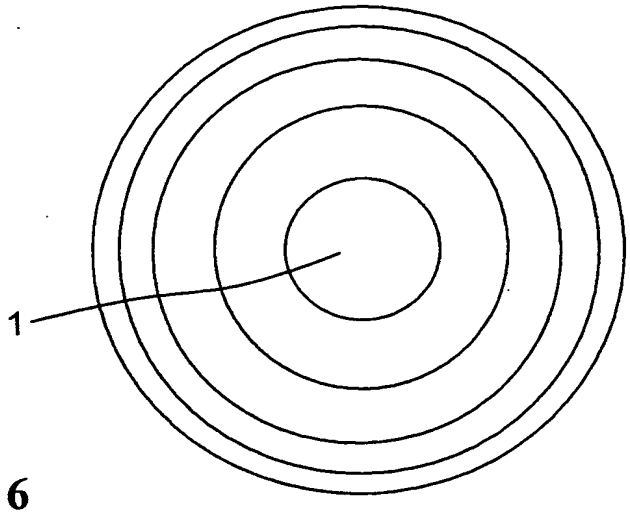

Fig. 6

1 inner circle

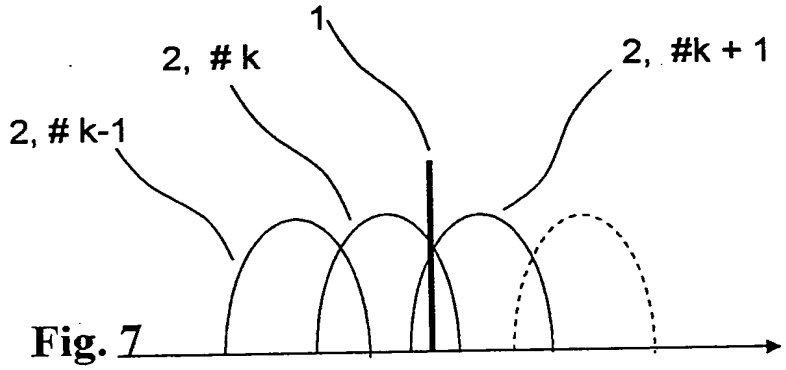

Fig. 7

1 - object
2 - Doppler filter

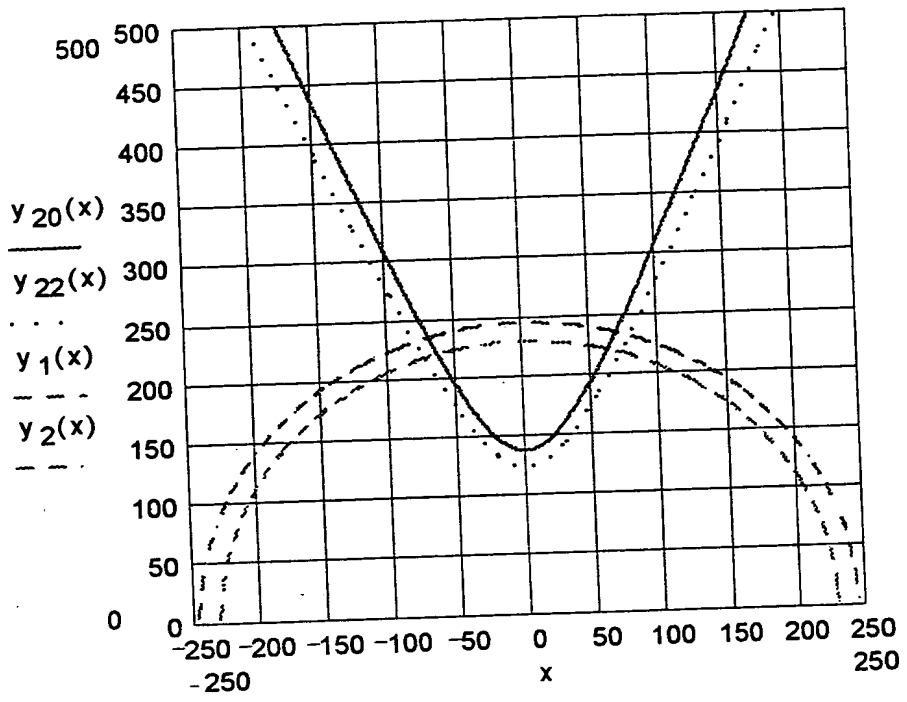
500
450
400
350
300
250
200
150
100
50
0
y 20(x)
y 22(x)
y 1(x)
y 2(x)
0
-250 -200 -150 -100 -50 0 50 100 150 200 250
250
-250
x

Fig. 8

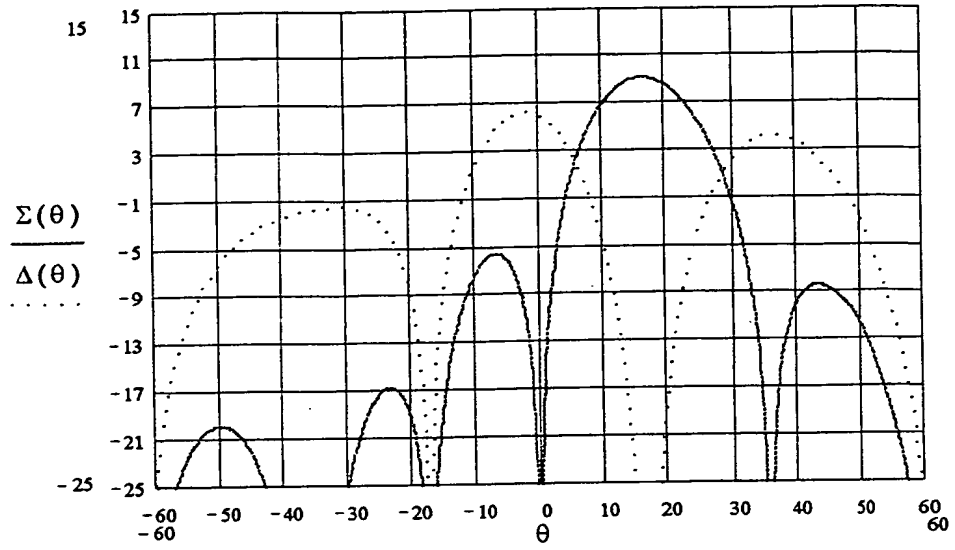

Fig. 9

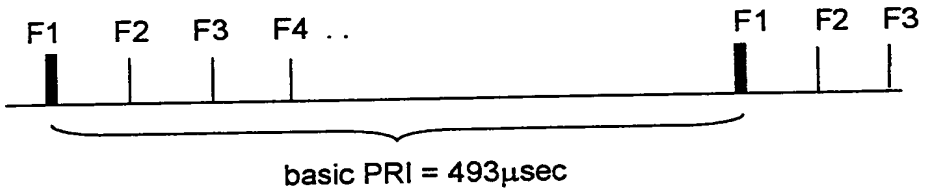

Fig. 10

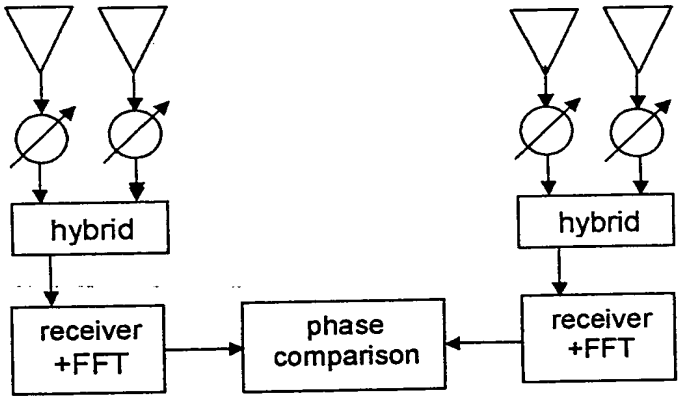

Fig. 11

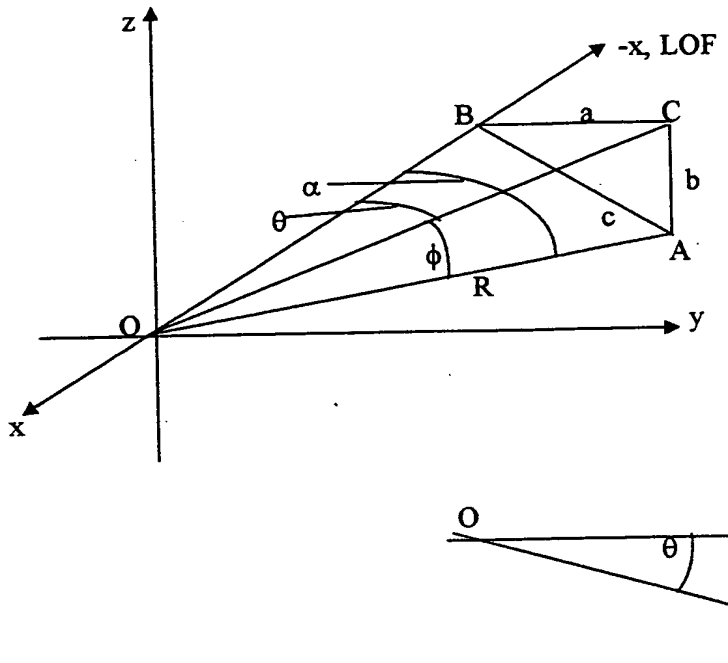

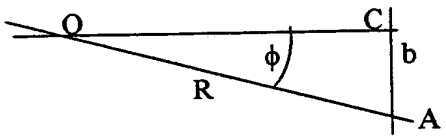

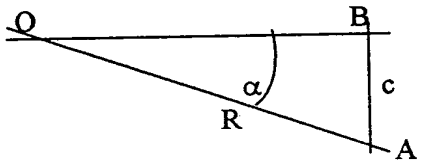

Fig. 12

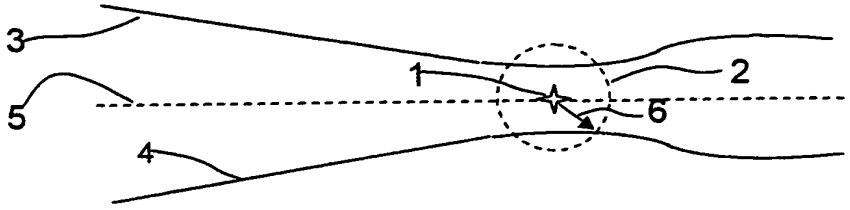

Fig. 13

1 - line of flight (LOF)
2 - safety circle
3 - terrain contour image
4 - terrain contour
5 - flight plane (FP)
6 - α_s, angle of safety circle (half head angle of safety cone)

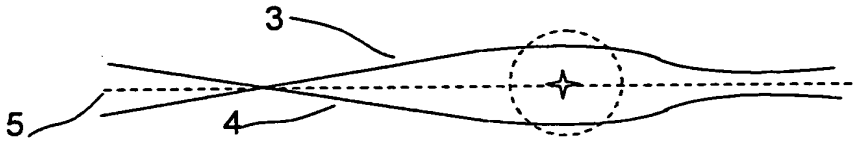

Fig. 14

(legend as for fig. 13 above)

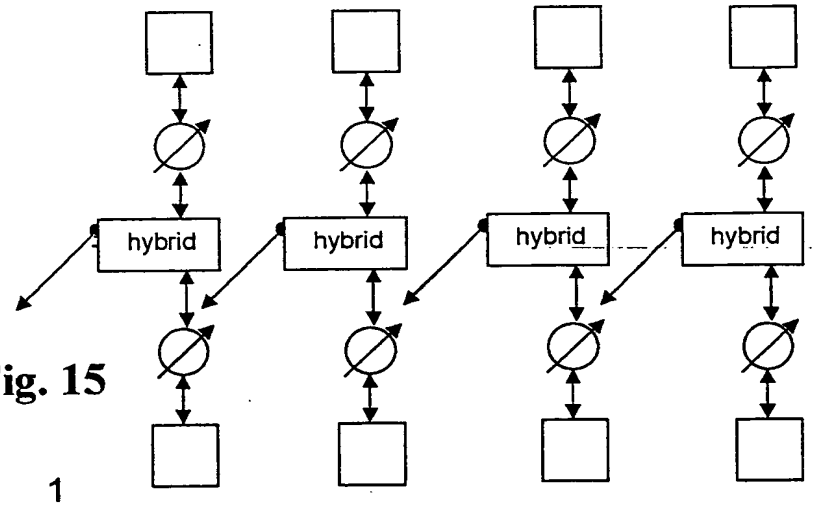

Fig. 15

1

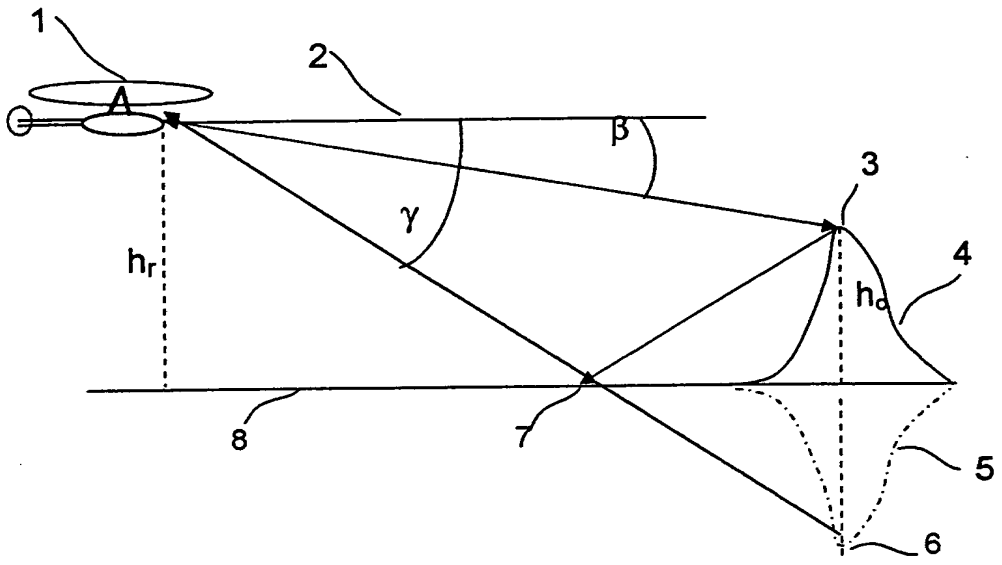

Fig. 16

1 - Aircraft
2 - Line of flight (LOF)
3 - Object's tip
4 - Object
5 - object's reflection image
6- object tip's reflection image
7 - reflection point
8 - terrain

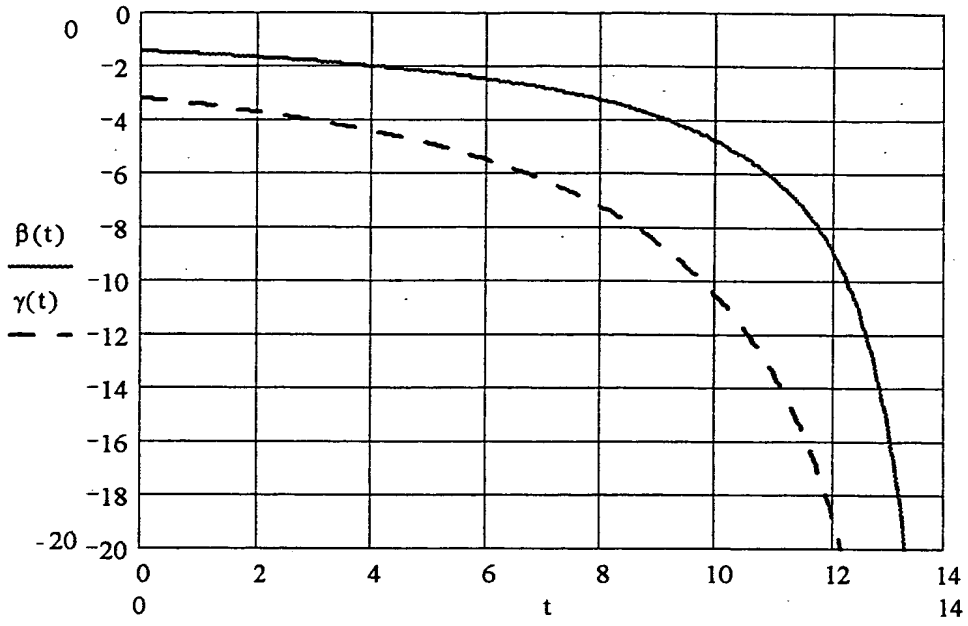

Fig. 17

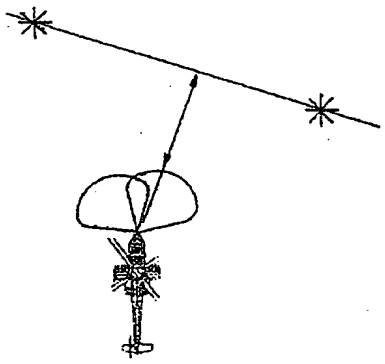

Fig. 18

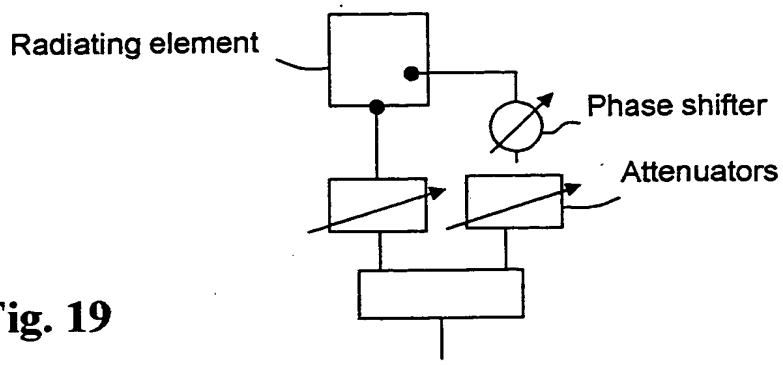

Fig. 19

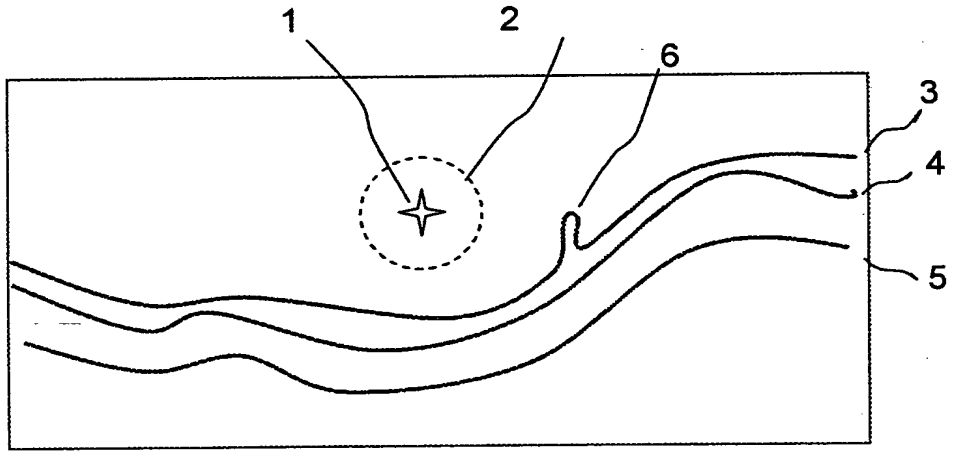

Fig. 20

1 - Line of sight (LOF) symbol
2 - safety circle
3 - Terrain contour at 1,000m
4 - Terrain contour at 500m
5 - Terrain contour at 200m
6 - point obstacle

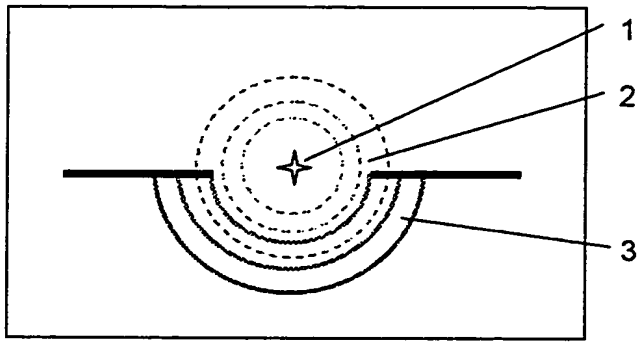

Fig. 21

1 - Line of flight (LOF) symbol
2- Safety circles
3 - contours

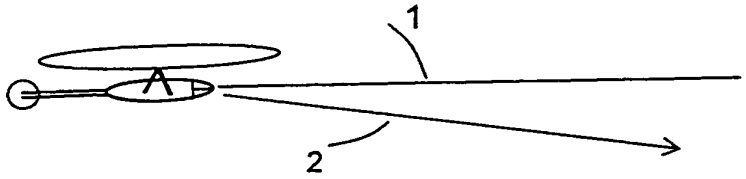

Fig. 22

1 - Aircraft's longitudinal axis
2 - Line of flight (LOF)